ICAARS 2018: Second International Conference on Advancements in Automation, Robotics and Sensing
PSG College of Technology, Coimbatore, India. 13-15 December 2018

Design and analysis of underactuated gripper using chebyshev's lambda mechanism with slip preventive strategy for fragile objects

Siril Teja Dukkipati[1],Mohammed Abdul Sulaiman [1], Kulpreet Singh Dhankar[1]

[1]Mechanical and Manufacturing Engineering, Manipal Institute of Technology, Manipal.
**sirilteja2012@gmail.com*

Abstract

This paper presents an underactuated gripper with slip prevention strategy for an unstructured human environment. In such environment the objects are of wide range in terms of size, shape and varying deformable properties. For the gripper to be able to grasp such objects an underactuated mechanism is implemented wherein chebyshev's lambda mechanism is used for linear motion of the fingers of the gripper. The work in the paper consists of positional analysis of lambda mechanism and underactuated fingers and kinetostatic analysis of the whole gripper. Using appropriately placed sensors and a novel slip prevention strategy the mathematical model of the gripper is used to lift objects with minimal amount of force without damaging them. The results show that the proposed gripper is suitable for unstructured human environments.

Keywords: *Chebyshev lambda, straight line mechanism, underactuation, slip, prevention, unstructured environments, fragile objects.*

1. Introduction

Gripper is a decisive part of a robot since it interacts with the environment and accomplishes the tasks. There has been extensive research done to produce a gripper with high dexterity to perform complex actions like mimicking human hands [1-4]. The human hand has 5 fingers and 21 degrees of freedom in total. Each finger is composed of three skeletons which are mainly used to perform three important functions including exploring, restricting and manipulating objects [6]. To perform dexterous moments with conventional grippers, additional links must be incorporated which makes the mechanism and control system complex. But by using underactuation, additional dexterity can be incorporated in grippers while keeping the design robust and simple [4][7][8].

In this paper a design of an underactuated gripper is proposed which adapts to the shape of the object. It consists of proximal, middle and distal phalanges which are connected to each other by revolute joints. The gripper is capable of performing two type of grasps namely power grasp and precision grasp. Power grasp is performed on objects of larger size and inertia and precision grasp on smaller sized objects and to perform precise motions. The power grasp is performed by proximal phalanx and middle phalanx. The precision grasp is performed by distal phalanx. The springs are used for restoring the phalanges to their initial state. In robotic applications, straight line pick and place motions are used for transferring work piece and are most advantageous in such applications because of accuracy of positioning the work piece [9] and thus provides great potential for high speed pick and place operations [10] [11]. Thus, the fingers of the proposed gripper are provided with straight line motion using chebyshev's lambda mechanism. Chebyshev's lambda straight line mechanism is chosen due to its simplicity and control. Since the paper aims at producing a gripper for unstructured human environment, the objects of such environment have wide variety of size, shape and varying deformation properties. The underactuated gripper is capable of grasping rigid objects of different size and shape by adapting in accordance with the object. Fragile objects pose great difficulty during grasp planning since if the forces applied on them are too large then the object can get damaged and if they are too small then the object can slip. Therefore, A slip prevention strategy is proposed for grasping the fragile objects by applying precise forces to grasp the object.

2. Mathematical Modelling

2.1. Lambda positional analysis

The lambda mechanism developed in this study is a nearly straight-line mechanism, rather than a straight-line mechanism. There is a deviation from straight line trajectory, however small it may be. A detailed positional analysis including deviation prediction of the mechanism is discussed below.

Fig.1a shows the configuration of the linkages of the lambda mechanism. The pin joints are marked with a circle. Consider origin at O and link lengths as shown in Fig.1a. The link OC is coupled with the gear which in turn is meshed with the driver gear and the motor. A torque applied on the link OC translates to useful force in X direction at point D.

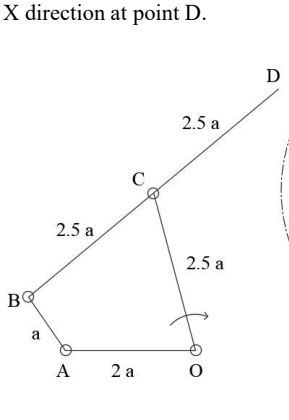

Fig.1a

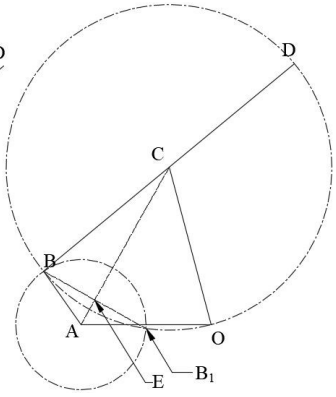

Fig.1b

Suppose that angle AOC is θ . We find the coordinates of all the other points including our point of interest D. By finding the coordinate functions of Point D in terms of θ w.r.t to the local origin O, we find the deviation of the mechanism from the true straight line. The coordinates of the points A and C are (-2a,0) and (-2.5a Cosθ, 2.5a Sinθ).

To find out the coordinates of point B, we can solve equations of both the circles drawn with centers A and C with radii 'a' and '2.5a' respectively. Alternatively, we use the vector analysis after finding the point E.

Hence,

$$x_B = \frac{a(25\cos^2\theta + 7.5\cos\theta - 31)}{20.5 - 20\cos\theta} - \sqrt{\frac{17 - 100\cos^2\theta + 60\cos\theta}{(42 - 40\cos\theta)(10.25 - 10\cos\theta)}}(2.5a\sin\theta)$$

$$y_B = \frac{a(12.5\sin\theta + 25\sin\theta\cos\theta)}{20.5 - 20\cos\theta} + \sqrt{\frac{17 - 100\cos^2\theta + 60\cos\theta}{(42 - 40\cos\theta)(10.25 - 10\cos\theta)}}(2a - 2.5a\cos\theta) \quad (1)$$

Hence, coordinates of D will be the reflection of B about C.

$$x_D = 2x_C - x_B \quad ; \quad y_D = 2y_C - y_B$$

Where, $(x_C, y_C) = (-2.5a\cos\theta, 2.5a\sin\theta)$ deviation of point D in Y direction is plotted against the input angle θ in Fig.2. The range of deflection is about 0.25 mm spanning across 40 degrees.

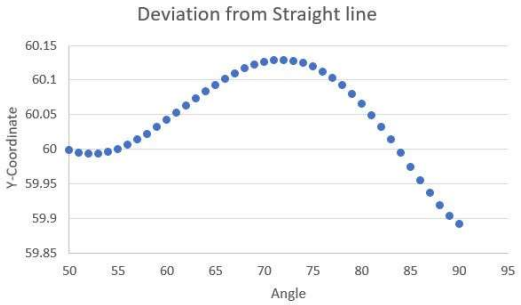

Fig.2

2.2. Lambda kinetostatic analysis

When torque is applied by the gear on the link OC, a reaction force is generated at point D whose X component is the useful force for object gripping.

Fixing the link OA to the ground, we resolve the components of the input torque τ and try to find out the output force F_i. This can be done by static force analysis of the mechanism at an arbitrary position θ. As represented in the Fig.2, the configuration angles $\theta, \alpha, \beta, \gamma$ are assumed known and the relation between the input torque and the output force is derived.

Both the parameters are related as,

$$F_i = \frac{\tau}{2.5a\sin\beta}\frac{\sin(\alpha+\beta)}{\sin\alpha} \quad (2)$$

And the best polynomial curve fitted relation between the angles in radians for $a = 15mm$ is given by

$$\alpha = (2.3316)\theta + (-2.0942)$$
$$\beta = (-0.6204)\theta^2 + (0.9703)\theta + (0.934)$$
$$\gamma = (0.6204)\theta^2 + (-1.9703)\theta + (2.2075)$$

With the above relations, the force F_i can be calculated with the knowledge of the torque applied by the driving mechanism and the size of the object to be picked up. Object size can be predicted by the configuration of the phalanges by some angle feedback mechanism such as a potentiometer.

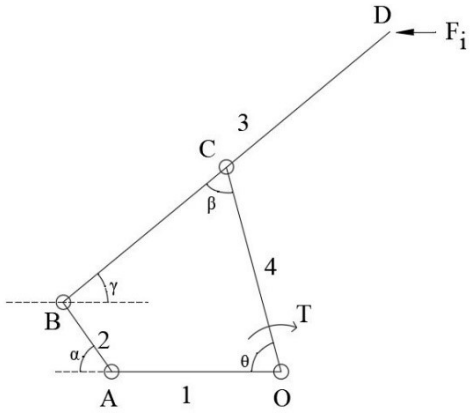

Fig.3

2.3. Finger positional analysis

Finger design in this study is restricted to only 1 extra degree of freedom to minimize functional failures due to singularities in mechanism. The object principal diameter and the velocity of approach of the finger towards the object can be found out from this study. Proceeding in the same lines as in 2.1, with a local origin setup at O, the coordinates of points A, B, F, E can be easily found out. The coordinate of point D can be derived as follows, considering the link lengths OA=30mm, AF=75mm, CD=25mm, OF=15mm, FE=ED=DB=30mm.

$$x_D = (-15\cos\phi - 15) + (60 - 30\sin\phi)\sqrt{(\frac{30}{d})^2 - 0.25}$$

$$y_D = (15\cos\phi + 45) - (-30 + 30\cos\phi)\sqrt{(\frac{30}{d})^2 - 0.25} \quad (3)$$

Where, $d = \sqrt{(30 - 30\cos\phi)^2 + (60 - 30\sin\phi)^2}$ which is the distance between the points E an d B.

Now, ψ can be found out easily by calculating the slope of the line ED. (4)

$$\psi = \operatorname{atan}\left(\frac{y_D - 15 - 30\sin\phi}{x_D + 30\cos\phi}\right)$$

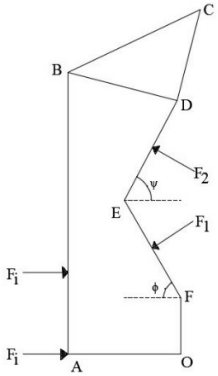

Fig.4

2.4. Finger static force analysis

Stability analysis of the object under grasp is the main aim of this section. F_1 and F_2 are the reaction forces on the finger structure applied by the object. The input force F_i from the lambda mechanism force analysis i.e. 2.2 is used here. Also, the relation between the angles ψ and ϕ from 2.3 is used. Forces on both the principal axes must sum up to nil.
Hence,

$$F_x = -F_1 sin\phi - F_2 sin\psi = 2F_i$$
$$F_y = -F_1 cos\phi + F_2 cos\psi = 0$$

Solving these equations, we get

$$F_1 = \frac{F_i}{(\sin\phi + \cos\phi\tan\psi)}$$

$$F_2 = \frac{F_i}{(\sin\psi + \cos\psi\tan\phi)} \quad (5)$$

Fig.5a and 5b shows the variation of the forces F_1 and F_2 with angles ϕ and ψ.

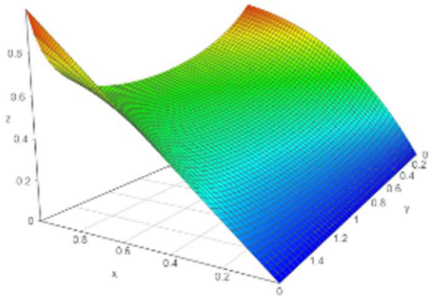

Fig.5a $(x, y, z) = (\phi, \psi, F_1)$

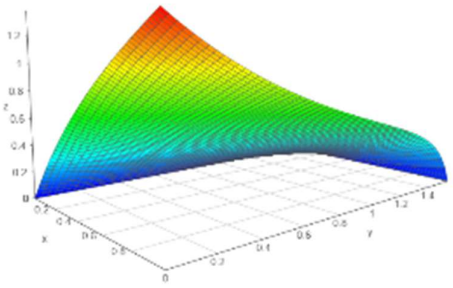

Fig.5b $(x, y, z) = (\phi, \psi, F_2)$

The gripper mimics the human finger and consists of proximal, middle and distal phalanges which are connected to each other by revolute joints. Thus, using this design, it is able to perform a power and precision grasp. Using Chebyshev's lambda mechanism, a straight-line motion is established. The mechanism is driven by a spur gear train which is driven by an electric motor. Positional encoders are located at particular joints to allow a real time positional and kinetostatic model of the gripper to be constructed. Force sensitive resistors are used at the distal phalanges to ascertain the forces being applied by the gripper on the object. Optical sensors are used on the phalanges to detect the slip of the objects. The optical sensors are required for to implement the slip prevention strategy which will be discussed in the later sections.

2.5. Lambda mechanism dynamic modelling

Lagrangian mechanics is used to model the lambda mechanism and its torque requirement for actuation. The Lagrange equation of the system has been solved using MATLAB. Considering only the masses and inertias of the links, this analysis has been done. The angle θ can be obtained by the feedback from the positional encoder fitted to the motor. It's angular velocity and acceleration can be calculated from the knowledge of θ. The code is presented below.

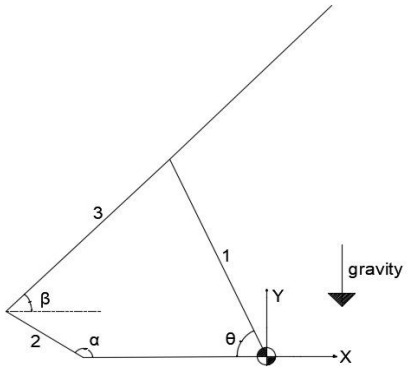

Fig.6 Line Diagram for modelling.

```
syms dpl ;                                          % density per unit length of the link
syms a ;                                            % chebyshev link parameter
syms theta theta_dot theta_dotdot ;                 % characteristic angle of the mechanism
syms T ;    % Motor torque
syms g ;    % gravity

A = 2.5*sin(theta) ; % A,B,x,y are the functions of theta used for finding alpha and beta
B = 2*cos(theta)-0.6 ;
y = ((2*A*B-5*A)+sqrt( (5*A-2*A*B)*(5*A-2*A*B) - 4*(5*B-7.25)*(1-A*A-B*B)))/(10*A-14.5);
x = A - (2.5*y) ;
alpha = asin(x);
alpha_dot =  theta_dot*(((5*cos(theta))/2 + (5*((25*cos(theta))/2 + 10*sin(theta)^2 -
5*cos(theta)*(2*cos(theta) - 3/5) - (((25*cos(theta)*sin(theta))/2 - 4*sin(theta)*(2*cos
(theta) - 3/5))*(40*cos(theta) - 41) - 40*sin(theta)*((25*sin(theta)^2)/4 + (2*cos(theta)
- 3/5)^2 - 1) + 2*((25*sin(theta))/2 - 5*sin(theta)*(2*cos(theta) - 3/5))*((25*cos
(theta))/2 + 10*sin(theta)^2 - 5*cos(theta)*(2*cos(theta) - 3/5)))/(2*(((25*sin(theta))/2
- 5*sin(theta)*(2*cos(theta) - 3/5))^2 + (40*cos(theta) - 41)*((25*sin(theta)^2)/4 +
(2*cos(theta) - 3/5)^2 - 1))^(1/2))))/(2*(25*sin(theta) - 29/2)) + (125*cos(theta)*
((((25*sin(theta))/2 - 5*sin(theta)*(2*cos(theta) - 3/5))^2 + (40*cos(theta) - 41)*
((25*sin(theta)^2)/4 + (2*cos(theta) - 3/5)^2 - 1))^(1/2) - (25*sin(theta))/2 + 5*sin
(theta)*(2*cos(theta) - 3/5)))/(2*(25*sin(theta) - 29/2)^2))/(- ((5*sin(theta))/2 - (-
(125*sin(theta))/2 + 5*(((25*sin(theta))/2 - 5*sin(theta)*(2*cos(theta) - 3/5))^2 +
(40*cos(theta) - 41)*((25*sin(theta)^2)/4 + (2*cos(theta) - 3/5)^2 - 1))^(1/2) + 25*sin
(theta)*(2*cos(theta) - 3/5))/(50*sin(theta) - 29))^2 + 1)^(1/2)) ;

p1x = -1.25*a*cos(theta) ;                          % x-position of link 1
p1y = 1.25*a*sin(theta) ;                           % y-position of link 1
p2x = -2*a + (a*0.5*cos(alpha)) ;                   % x-position of link 2
p2y = a*0.5*sin(alpha) ;                            % y-position of link 2
p3x = -2.5*a*cos(theta) ;                           % x-position of link 3
p3y= 2.5*a*sin(theta) ;                             % y-position of link 3
v1x = 5*0.25*a*sin(theta)*theta_dot ;               % x-velocity of link 1
v1y = 5*0.25*a*cos(theta)*theta_dot ;               % y-velocity of link 1
v2x = -0.5*a*sin(alpha)*alpha_dot ;                 % x-velocity of link 2
v2y = 0.5*a*cos(alpha)*alpha_dot ;                  % y-velocity of link 2
v3x = 2.5*a*sin(theta)*theta_dot ;                  % x-velocity of link 3
v3y = 2.5*a*cos(theta)*theta_dot ;                  % y-velocity of link 3

syms M1 M2 M3 ;                                     % M is the mass of the link
M1 = dpl*2.5*a ;
M2=dpl*a ;
M3=dpl*5*a ;

KE = 0.5*M1*( v1x^2 + v1y^2) + 0.5*M2*( v2x^2 + v2y^2) + 0.5*M3*( v3x^2 + v3y^2) ;
                                                    % Kinetic Energy of the system
PE = M1*g*p1y + M2*g*p2y + M3*g*p3y ;               % Potential Energy of the system


pKEptheta_dot = diff(KE,theta_dot) ;                % partial diff. of KE w.r.t theta_dot
ddtpKEptheta_dot = diff(pKEptheta_dot,theta)*theta_dot+ diff(pKEptheta_dot,theta_dot)
*theta_dotdot ;
                                                    % diff of the above term w.r.t time
pKEptheta = diff(KE,theta);                         %  partial diff. of KE w.r.t theta
pPEptheta = diff(PE,theta);                         % partial diff. of PE w.r.t theta_dot
```

```
T =  ddtpKEptheta_dot - pKEptheta + pPEptheta ;                    % External torque
display(T);
```

In addition to this inertial torque requirement, we should also take into account, the torque requirement of the finger actuation i.e. for F_i.

3. Slip prevention strategy and experimental procedure

In order to devise a slip strategy, the gripping process of humans was analyzed. 3 parameters were used to judge this, the grip force, which is the amount of force exerted by the fingers on the object. The load force, which is the force exerted by the fingers due to friction and the position or the height gained by the object. Finally, all these were plotted on a graph which along with the slip ratio which is the ratio of grip force to load force. The idea is to quantify the initial grip force and its rate of change for a particular object. This ratio will further be used to calculate the grip force which should be applied on an object to ensure a slip free grasp [13]. Humans use different slip ratios for different types of objects. For light weight deformable objects like fruits, human's use a lower value of slip ratio to avoid damaging them, whereas reverse is true for higher weight objects [12]. Thus a strategy of selecting a slip ratio which is high enough to ensure an object doesn't slip is proposed. In addition to this it is ensured that the slip ratio is low enough to now damage the object.

In sufficient literature it was pointed out that the grasp technique of adults was very different from that of children [11]. Thus we conducted tests on both children and adult to analyze which one is more suitable to be employed for slip prevention. An object with weight 200 g was lifted and the graphs were plotted as shown in Fig.7.

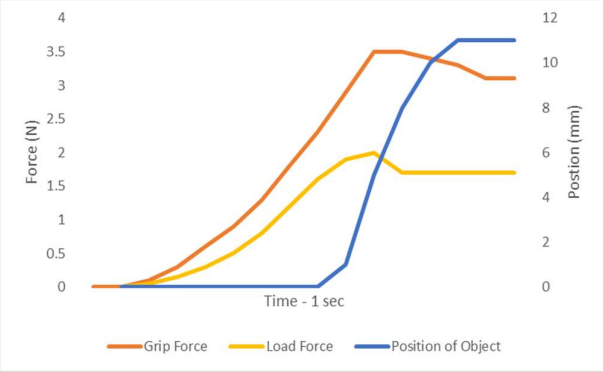

Fig.7 Force variation in adult grasp

As can be seen from Fig.7, for adults after both the fingers come in contact with the object the grip force is gradually increased. The load force increases in parallel with the grip force. Once the object starts to lift up the load force increases to a maximum value and then becomes constant. During this the slip ratio increases to a maximum and then decreases again. Thus there is a parallel increase of grip force and load force.

For children, the increase of grip force and load force is sequential rather than parallel as is evident from Fig.8. Children first apply a certain amount of grip force before actually applying any load force. This may be accredited to their lack of experience [11]. This technique may be useful in unstructured environments since no prior data is available about the object.

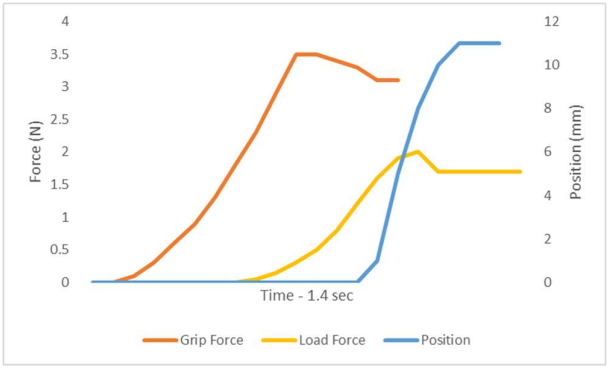

Fig.8 Force variation in child

This technique of sequentially applying forces has a major flaw. If there is no cap on the maximum amount of grip force being applied, then it may damage an object. Thus we conducted an experiment to determine the maximum initial grip force wherein a person is asked to lift different objects. Force sensors are fixed on the fingers of the hand to record the amount of forces applied. During the experiment the human is blind folded so that he is not able to approximate the force required by seeing the object. Initially he is only asked to make contact with the object and announce whether he is ready to lift the object. The reading at this point indicates the minimum initial force which all the human hands apply on objects before lifting them irrespective of the weight. Then the human is asked to lift the object. The variation in force applied while lifting, which also includes multiple instantaneous slip events, is recoded and compared with the weight of the object. It is observed that this change of force is dependent on the type of object being lifted which is listed in the table.

Table 1

Objects	F_0	δF	Weight
Water Cup	1.25 N	0.01 N	240 gms
Egg	1.27 N	0.02 N	56 gms
Tomato	1.14 N	0.11 N	98 gms
Hammer	1.20 N	0.5 N	500 gms

Using the above experiment, the initial force which the gripper must apply can be approximated. The next challenge is to determine the rate at which the gripper must change its force to prevent slip of the object, when the initial applied force is not enough to lift the object. To determine this, an experiment is conducted wherein a human is asked to grip an empty cup. Water is poured in this cup at varying rates of flow as listed in the table. As expected, for a higher rate of flow the rate of change of applied force is higher.

Table 2

Rate of change of mass	δF
10 gms/sec	0.05 N
15 gms/sec	0.08 N
20 gms/sec	0.13 N
25 gms/sec	0.20 N

The selection of most optimal rate of change of force depends on 2 factors. The rate of change should not be too high as it can damage fragile objects, also it should not be too low otherwise objects of higher weight might slip off. In order to find the optimal rate of change of force, an experiment is conducted where in all the rates found in table 2 are applied on objects of table 1.

Table 3

δF	Outcome
0.05 N	Hammer, tomato, egg starts slipping.
0.08 N	Tomato, hammer starts slipping.

0.13 N	All objects are grasped.
0.20 N	Water cup is crushed.

From table 3 it was concluded that $\delta F = 0.13\ N$ was found to be most optimal wherein all objects can be gripped without slip and damage to the object.

4. Conclusion and further work

The work demonstrates that the proposed gripper can operate in an unstructured human environment. It can successfully use both precision and power grasp to lift objects. This is done by first mathematically modelling the gripper and then using this model along with the slip prevention policy to successfully lift an object. A rate of $\delta F = 0.13\ N$ is selected to lift an object, without damaging or letting it slip, based on experiments. During experiments it was found that the initial force applied by human hands was directly proportional to the size of the object. It is planned to incorporate this as well in the slip prevention strategy in future to make the gripper more robust.

Fig.9 Prototype of the proposed design

Fig.10 Flange in power grasp

Fig.11 Experimental Setup

Fig.12 Sensor Setup and variable mass experiment setup

Acknowledgement

This research is supported by Mars Rover Manipal and Manipal Academy of Higher Education, Manipal.

References

[1] Wenzeng Zhang, Jie Sun, "A novel coupled and self-adaptive under-actuated multi-fingered hand with gear–rack–slider mechanism", Journal of Manufacturing Systems, Vol 31, PP- 42–49, 2012.

[2] M.G. Catalano1, G. Grioli1, E. Farnioli1, A. Serio1, C. Piazza and A. Bicchi, "Adaptive synergies for the design and control of the Pisa/IIT Soft Hand", The International Journal of Robotics Research, Vol. 33(5), PP 768–782, 2014, DOI: 10.1177/0278364913518998.

[3] Daniel M. Aukes, Barrett Heyneman, John Ulmen, Hannah Stuart, Mark R. Cutkosky, Susan Kim, Pablo Garcia and Aaron Edsinger, "Design and testing of a selectively compliant underactuated hand", *The International Journal of Robotics Research* 2014 Vol 33: 721.

[4] S.C. Jacobsen, E.K. Iversen, D.F. Knutti, R.T. Johnson, K.B. Biggers," DESIGN OF THE UTAH/M.I.T. DEXTROUS HAND", Center for Engineering Design, University of Utah.

[5] Bin Gao, Long Lei, Shijia Zhao, Ying Hu, Jianwei Zhang, "A Novel Underactuated Hand with Adaptive Robotic Fingers", Proceedings of the IEEE, International Conference on Information and Automation, Ningbo, China, August 2016.

[6] Wu LiCheng, Giuseppe Carbone, Marco Ceccarelli, "Designing an underactuated mechanism for a 1 active DOF finger operation.", Mechanism and Machine Theory Vol 44, 336–348, 2009.

[7] KUAT TELEGENOV, YEDIGE TLEGENOV, ALMAS SHINTEMIROV, "A Low-Cost Open Source 3-D-Printed Three-Finger Gripper Platform for Research and Educational Purposes.", IEEE Access, the journal of rapid open access publishing. DOI:*10.1109/ACCESS.2015.2433937.*

[8] Y. Gene Liao, "Design and Analysis of a Modified Scott Russell Straight-Line Mechanism for a Robot End-Effector.", journal of applied science & engineering technology 2011.

[9] J. H. Seo, H. J. Yim, J. C. Hwang, Y. W. Choi, and D. Kim. "Dynamic load analysis and design methodology of LCD transfer robot", Journal *of Mechanical Science and Technology*, vol. 22, pp. 722-730, 2008.

[10] T. Huang, P. F. Wang, J. P. Mei, X. M. Zhao, and D. G. Chetwynd, "Time minimum trajectory planning of a 2-DOF translational parallel robot for pick-and-place operations", Annals *of the CIRP,* vol. 56, no. 1, pp. 365-368.

[11] H. Forssberg, A.C. Eliasson a, H. Kinoshita, R.S. Johansson, and G. Westling, "Development of human precision grip I: Basic coordination of force", Exp Brain Res (1991), Vol 85, pp. 451-457.

[12] Michael Stachowsky, Julie Vale, Hussein A. Abdullah, and Medhat Moussa, "A Human-Inspired Real-Time Grasp Force Selection Policy Based on Load-Grip Force Coupling", *International Journal of Mechanical Engineering and Robotics Research Vol. 4, No. 4, October 2015*

[13] R.S. Johansson and G. Westling, "Coordinated isometric muscle commands adequately and erroneously programmed for the weight during lifting task with precision grip", Exp Brain Res (1988) 71:59-71